Energy, Mines and Resources Canada
Earth Physics Branch

Énergie, Mines et Ressources Canada
Direction de la physique du globe

Geomagnetic Service of Canada

Service géomagnétique du Canada

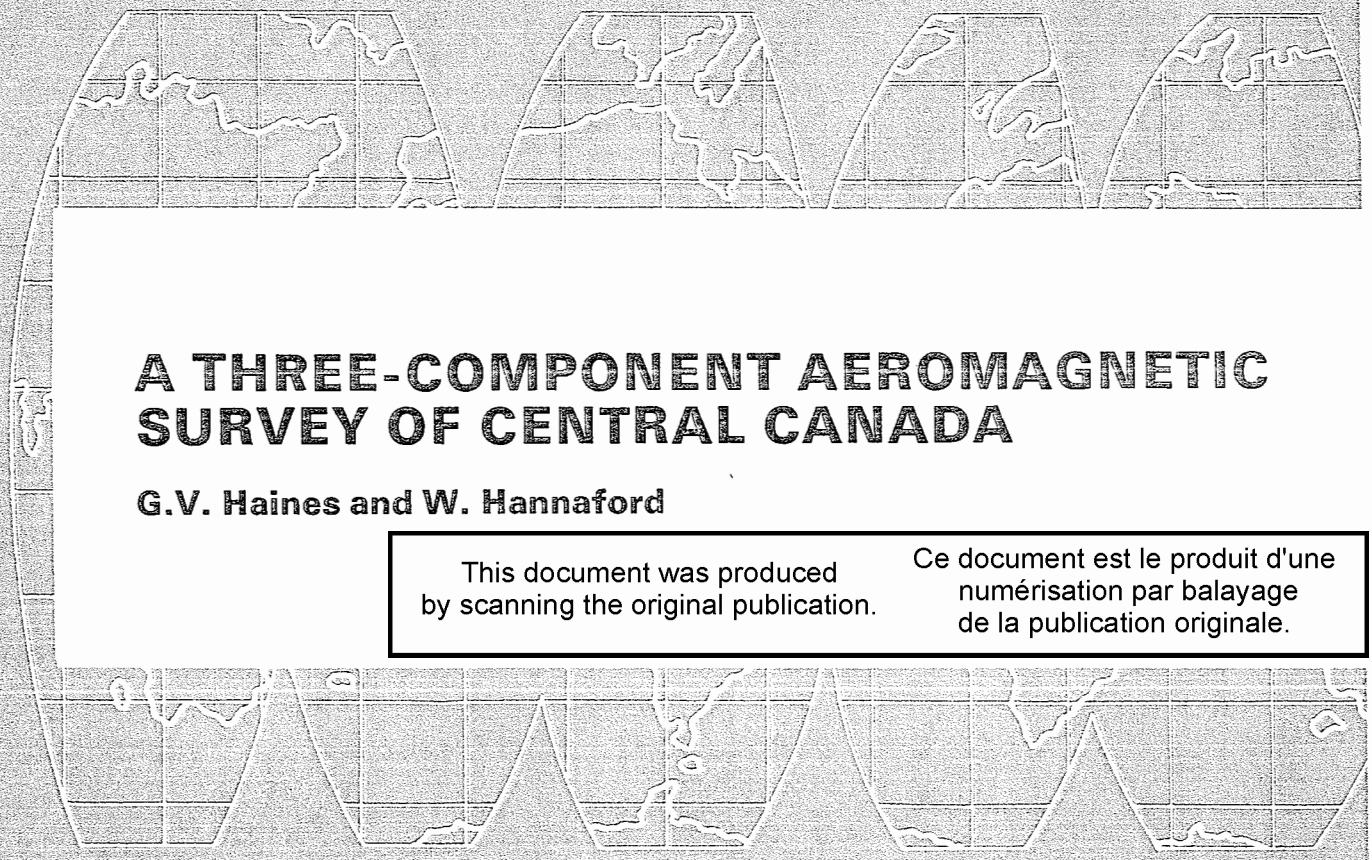

A THREE-COMPONENT AEROMAGNETIC SURVEY OF CENTRAL CANADA

G.V. Haines and W. Hannaford

This document was produced by scanning the original publication.

Ce document est le produit d'une numérisation par balayage de la publication originale.

Geomagnetic Series
Number 13
Ottawa, Canada 1978

Série géomagnétique
Numéro 13
Ottawa, Canada 1978

Energy, Mines and Resources Canada
Earth Physics Branch
1 Observatory Crescent
Ottawa Canada
K1A 0Y3

Énergie, Mines et Ressources Canada
Direction de la physique du globe
1 Place de l'Observatoire
Ottawa Canada
K1A 0Y3

Geomagnetic Service of Canada

Service géomagnétique du Canada

A THREE-COMPONENT AEROMAGNETIC SURVEY OF CENTRAL CANADA

G.V. Haines and W. Hannaford

Geomagnetic Series
Number 13
Ottawa, Canada 1978

Série géomagnétique
Numéro 13
Ottawa, Canada 1978

© Minister of Supply and Services Canada 1978

Available by mail from

Printing and Publishing
Supply and Services Canada
Hull, Québec, Canada, K1A 0S9

Earth Physics Branch,
Energy, Mines and Resources Canada,
1 Observatory Crescent,
Ottawa, Canada K1A 0Y3

or through your bookseller

Catalogue No. M74-32/13 Price: Canada: $1.00
ISBN 0-660-00714-2 Other countries: $1.20
ISSN 0704-3015

Price subject to change without notice.

© Ministre des Approvisionnements et Services Canada 1978

En vente par la poste:

Imprimerie et Édition
Approvisionnements et Services Canada
Hull, Québec, Canada, K1A 0S9

Direction de la physique du globe,
Énergie, Mines et Ressources Canada,
1 Place de l'Observatoire,
Ottawa, Canada K1A 0Y3

ou chez votre libraire.

N° de catalogue M74-32/13 Prix: Canada: $1.00
ISBN 0-660-00714-2 Autres pays: $1.20
ISSN 0704-3015

Prix sujet à changement sans avis préalable.

CONTENTS

Abstract - Résumé v

Introduction 1

The Magnetometer Systems 1

The On-board Minicomputer System 1

Navigation 2

Solution of Permanent and Induced Aircraft-field Corrections 3

Effect of Magnetometer Orientation 7

Swing-derived Corrections 8

Correction of Data 10

Consistency-derived Corrections for Z 11

Data Rejection for Magnetic Disturbance 13

Presentation of Data 13

Acknowledgments 15

References 15

ABSTRACT

A three-component airborne magnetic survey of Ontario, Manitoba, Keewatin, and parts of Quebec and Franklin was carried out in late 1974, at an average altitude of 3.5 km. The survey area is centered on the auroral zone, and so magnetic disturbances of high amplitude occurred frequently. These disturbances pose a serious problem to the determination of the internal geomagnetic field, and only data considered to be relatively free of disturbance fields are presented here. The data were averaged over 30 seconds of time, or approximately 3.5 km of flight track. The International Geomagnetic Reference Field (IGRF) was removed from these averages, and the resulting residuals plotted as profiles. A 3rd degree polynomial was fitted to the survey data by least-squares. Contour plots of the polynomial field minus the IGRF are given.

RÉSUMÉ

Un relevé aéromagnétique à trois composantes à été effectué au dessus de l'Ontario, du Manitoba, du Keewatin, et de certaines parties du Québec et du Franklin à la fin de 1974, à une altitude moyenne de 3,5 km. Le centre du relevé est situé dans la zone aurorale, si bien que des perturbations magnétiques de grandes amplitudes se produisent fréquemment. Ces perturbations présentent un problème majeur pour la détermination du champ géomagnétique interne. On ne presente ici que les données qui ont été enregistrées pendant les periodes tranquilles. Les données du relevé sont représentées sous forme de moyennes sur une periode de temps de 30 seconds, équivalent à une distance de 3,5 km. On a soustrait de ces données les valeurs du champ géomagnétique international de référence (International Geomagnetic Reference Field - IGRF), et les données résiduelles ont été tracées sous formes de profils. On a appliqué un polynome du 3^{e} degré aux données du relevé par la méthode des moindres carrés. On présente des cartes des lignes de contours du champ polynome duquel a été soustrait le IGRF.

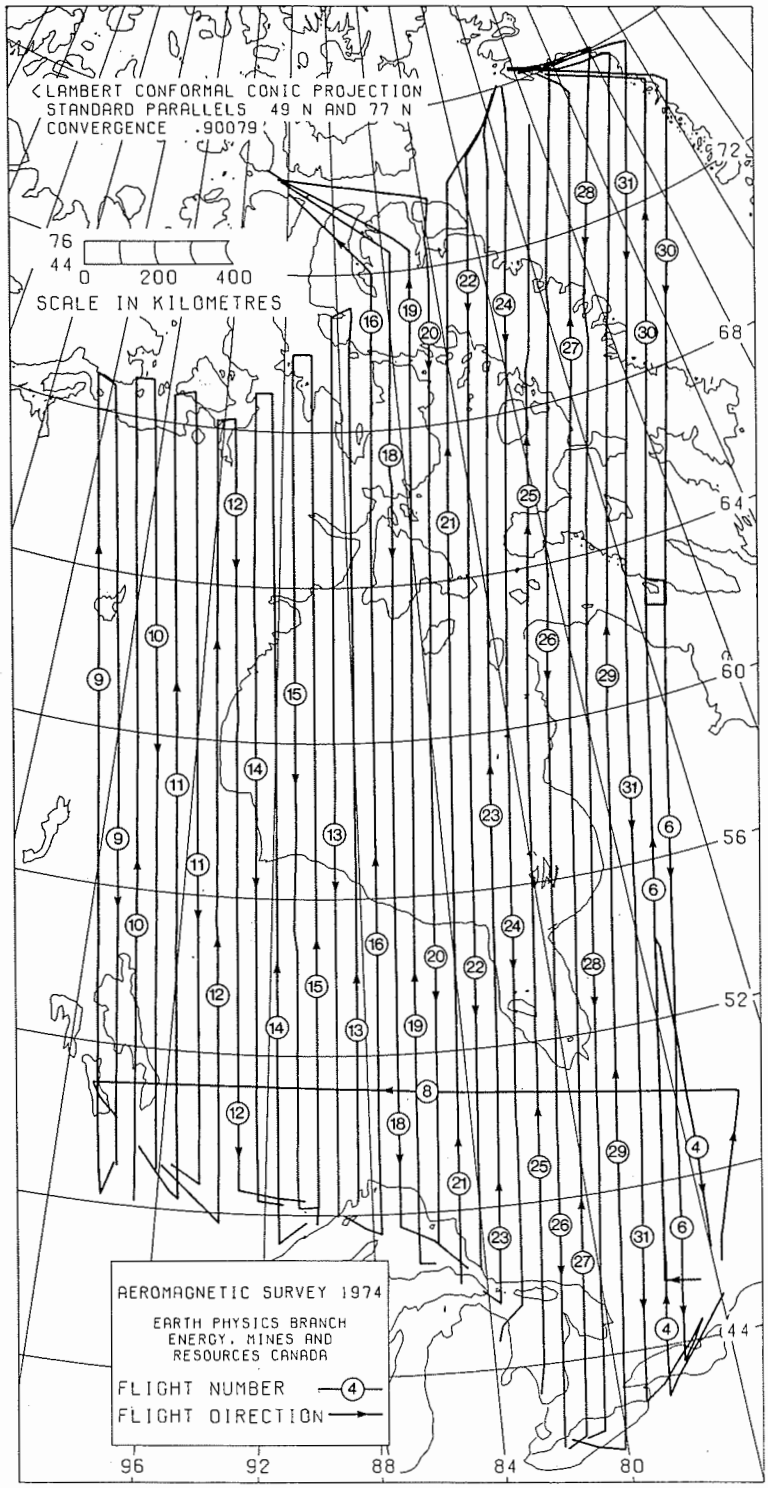

Figure 1. Flight lines of the Earth Physics Branch 1974 3-component aeromagnetic survey of Ontario, Manitoba, Keewatin, and parts of Quebec and Franklin. Flight numbers are circled and arrowheads indicate the direction of flight. The survey was carried out between September 19 and November 30, 1974, at an average altitude of 3.5 km.

A THREE-COMPONENT AEROMAGNETIC SURVEY OF CENTRAL CANADA

G.V. Haines and W. Hannaford

INTRODUCTION

In 1974, between September 19 and November 30, the Earth Physics Branch (EPB) carried out an airborne three-component magnetic survey over Ontario, Manitoba, Hudson Bay, the district of Keewatin, Baffin Island, Baffin Bay, and the western edge of Quebec. An index map of the survey flight lines is shown in Figure 1.

The aircraft used was a DC-6, chartered from Conair Aviation. Approximately 118,000 kilometres were flown, of which about 27,000 were test, ferry and calibration flights. The average flight-line spacing was 56 km (30 nautical miles), and the area covered was 5.4 x 10^6 km . Flight altitudes ranged from 1.8 to 4.9 km above sea level, the average being 3.5 km (11,400 feet).

THE MAGNETOMETER SYSTEMS

There were two magnetometers aboard the aircraft. One was a three-component fluxgate magnetometer which produces continuous analog signals for declination D, horizontal intensity H, and vertical intensity Z. The fluxgate sensors, mechanically linked to a gyro-stabilized platform, were mounted in the aft section of the main cabin. The other was a proton-precession magnetometer which produces digital samples of total intensity F_p every three seconds. The proton sensor was located in the end of a 3.5 metre tail boom extending from the rear of the fuselage.

The platform, magnetometers, and data-acquisition system are essentially as described by Haines and Hannaford (1974). Since then, however, a minicomputer has replaced digital counters as a means of computing five-minute averages of the geomagnetic elements. The minicomputer also performs several functions which are new to the system and will be described in the next section.

Another instrumental modification was the addition of a second output to the system which measures D_g, the angle between magnetic north and the directional gyro. The new output, which we call D_{lo}, follows D_g with less accuracy (approximately $\pm 2^o$) than does its counterpart D_{hi} ($\pm 0.\overline{06}^o$), but D_{lo} is unambiguous and covers an unlimited range by returning to zero when D_g reaches a multiple of 360^o, whereas D_{hi} can be ambiguous by a multiple of 10^o. This ambiguity arises because the angle D_g is multiplied by a gear ratio of 36:1 at the D_{hi} transmitter synchro in order to achieve the higher accuracy. Hence D_g is determined within 0.06^o by adding D_{hi} to the proper multiple of 10^o as determined from D_{lo}.

The elements D_{hi}, H, and Z and the analog conversion of F_p were recorded on strip-charts on a time-base of 1 in/min and at selectable sensitivities, normally 100 nT/in for H, Z, and F_p and 1^o/in for D_{hi}. Digital samples of D_{lo}, D_{hi}, H, and Z were taken every three seconds and recorded, along with F_p, on magnetic tape.

THE ON-BOARD MINICOMPUTER SYSTEM

Subsequent to the 1970 survey (described by Haines and Hannaford, 1974) the EPB airborne magnetic survey equipment was interfaced to an Interdata Model 70 minicomputer which now performs data averaging and several other in-flight functions. Peripheral devices of the minicomputer system include a CRT data screen, keyboard, printer, plotter, and cassette tape unit with read/write capability on three transports.

Each set of geomagnetic data which is recorded on magnetic tape is simultaneously fed into the computer. A byte-by-byte check of the synchronously input quantities is done and those containing non-numeric bytes are rejected. The computer counts the number of such bytes found in one sampling cycle, and flashes that number on the data screen. Successive half-minute and five-minute averages of each geomagnetic element are computed at the end of each averaging

interval. The five-minute averages and corresponding mean GMT are printed and also displayed on the data screen where they replace the previous set. The half-minute averages are recorded on cassette tape.

With each new set of averages the computer calculates total intensity F_f from the fluxgate measurements, and displays the difference $F_f - F_p$ on the data screen. If this difference exceeds a selected limit the value on the data screen flashes on and off to signal a malfunction of one of the magnetometers or the presence of an abnormal magnetic field at one of the sensors. A similar visual alarm is triggered if D_{hi} lags out of step with D_{lo}.

The computer also receives, every minute, instantaneous values of aircraft ground speed and drift angle from a Canadian Marconi CMA 621-A Doppler Navigator and of heading angle from the directional gyro of the fluxgate stabilization system. This gyro's deviation from grid north is monitored by taking frequent astro observations with a stabilized periscopic sextant. The gyro deviation and drift rate are fed into the computer manually. Initial latitude and longitude are also input manually before takeoff, and are subsequently updated in flight by the computer every minute, using the Doppler and heading information mentioned above. The sixty most-recent one-minute positions are stored in memory for access by other programs. Any error which accumulates in the succession of computed one-minute positions can be removed by keying in an accurate set of latitude, longitude and time. The next position computation is adjusted accordingly, and the accurate fix, the corresponding computed position, the distance between the two, and real time are recorded on the printer.

The table of aircraft positions at each minute during the past hour can be accessed (at the operator's option) by the computer for the computation of an astronomical azimuth at a specified time. Otherwise the operator provides the appropriate latitude and longitude via the keyboard. The astronomical coordinates required for azimuth computations are interpolated by the computer from the ephemeris values at 00:00 and 24:00 GMT of that day, which must of course be previously entered. The emphemeris information for up to ten different astronomical bodies can be stored in the computer at one time.

The azimuth computations are required for monitoring the directional gyro as mentioned above. The same computer program also yields the altitude of the observed star, from which a position line may be obtained using the Marcq St.-Hilaire altitude intercept method (Bowditch 1962), or conversely the tilt of the sextant can be checked if position is accurately known.

The computer also uses its one-minute positions to determine Z and H residuals and plot them versus distance to produce anomaly profiles in real time. The reference field which is subtracted from the half-minute Z and H averages to obtain the corresponding residuals is a third-degree polynomial which was fitted by least squares to the IGRF in the survey area.

The position computed for the centre of the latest five-minute averaging interval and the corresponding number of nautical miles flown from a selected starting point (usually takeoff) are displayed on the data screen along with the five-minute averages of D_g, H, Z, F_p, magnetic heading ψ, and gyro heading ψ_g. This information is written into the log by the operator and is also recorded on the printer together with the averages of $F_f - F_p$ and $D_{hi} - D_{lo}$.

The latest set of all instantaneous values which the computer receives in a regular cycle is displayed digitally on the data screen once per minute. These values are scanned by the operator but they are not logged unless there appears to be something wrong. In such a case the operator can command a print-out of the complete set.

The computer system provides an on-line means of editing and processing the data and then recording them in convenient form on cassette, printer and plotter. It also serves as an independent navigation computer and as a continuous monitor of the performance of the magnetometers and the consistency of the data. However, it does not perform exclusively any function which is vital to the output and acquisition of raw data from the magnetometers, stabilized platform, or navigation equipment.

NAVIGATION

Two navigators were on duty through each flight. The Doppler system mentioned in the preceding section gave a continuous indication of ground speed and drift angle at the navigator's station. In addition the doppler has its own analog computer which indicates the distance flown along a desired track and the aircraft's distance to the left

or right of that track. The four Doppler output quantities were logged every ten minutes along a survey line.

The principal instrument of navigation aboard the aircraft was a Litton LTN-51 Inertial Navigation System (INS). The control unit of this system has a keyboard and two digital displays for the input and output of navigation information. Before takeoff, an initial alignment procedure is completed, during which the navigator inputs values of latitude and longitude for the aircraft's position at that time, for its final destination, and for up to nine waypoints along the desired flight path. In flight the INS yields the following information as selected by the navigator: true track angle and ground speed, true heading and drift angle, cross-track and track angle errors, latitude and longitude, distance and time to next waypoint, wind direction and velocity, and desired track angle to next waypoint. The values presented on the digital display are updated every second in time. The INS cross-track error output is also available as an analog signal which can be coupled to the autopilot's steering control to keep the aircraft on course automatically. Latitude and longitude were logged ever ten minutes during flight, along with other INS information selected by the navigator. In addition, the aircraft's actual latitude and longitude were determined by map reading approximately once per hour when visual position fixes were available. Any error which accumulates in the position output of the INS can be removed by inserting the correct information and giving an "update" command. The INS was normally updated when visual fixes showed an error greater than two or three nautical miles.

At the end of each flight the INS position, which may have been updated one or more times, can be compared with the accurately known position in which the aircraft is parked. The latter position can be fed into the INS which, on command, will then yield the "terminal error", i.e. distance between the true and INS positions. Similarly the INS can also be commanded to yield the final position which it would have indicated if no in-flight updates had been performed, and also the "trip error", i.e. distance between the true and uncorrected final position.

The terminal error depends primarily on the last update of the flight. Of 8 flights ending in the northern part of the survey, the terminal error was 7.6 ± 1.3 km. Of 16 flights ending in the southern part the terminal error was 4.6 ± 1.0 km. The standard deviation of the terminal errors was about 4 km in each case.

The trip error was significantly larger when the INS pre-flight alignment was performed at high latitudes (Resolute Bay 74.7°N and Thule 76.5°N). On 8 flights originating in the northern part of the survey area, and ranging in duration from 9.1 to 11.4 hours, the trip error rate was 2.3 ± 0.3 km/hr. On 16 flights originating in the southern part of the survey area, and ranging from 7.8 to 13.8 hours in duration, the trip error rate was 0.8 ± 0.2 km/hr. The standard deviation of the trip error rates was about 0.8 km/hr in each case.

All information logged by the navigator during flight was used to back-plot each track, and produce a listing of positions normally at time intervals of ten minutes and when the aircraft changed heading. The absolute accuracy of a position is estimated on the basis of the terminal errors to be about 5 km in the southern part of the survey area and about 8 km in the northern part. The relative accuracy within a flight is estimated on the basis of the trip errors to be less than 1 km/hr in the southern areas and less than 3 km/hr in the northern areas.

In assigning positions to times not in the listing, it was assumed that the ground speed was constant and the aircraft followed a great-circle path between the listed positions. The error introduced by this procedure is estimated to be less than 1 km when the time interval between listed positions is 10 minutes. Of course this error is zero at the listed positions and increases toward the centre of the interval.

SOLUTION OF PERMANENT AND INDUCED AIRCRAFT-FIELD CORRECTIONS

Let P denote the component of the earth's magnetic field along the forward axis of the aircraft, Q the component along the right traverse axis, and Z the vertical downward component. Let P', Q', and Z' be the respective components of the "apparent" field, i.e. the aircraft's and earth's field combined. Then the corrections to P', Q' and Z' due to both induced and permanent magnetic fields are given by:

$$P - P' = aP + bQ + cZ + P_0 \qquad 1$$

$$Q - Q' = dP + eQ + fZ + Q_0 \qquad 2$$

$$Z - Z' = gP + hQ + kZ + R_0 \qquad 3$$

If there is little variation in Z over the calibration areas, the contributions due to c, f, and k cannot be separated from those due to P_0, Q_0, and R_0. In this survey, for example, the Z variation was less than 5%. Hence we redefine the permanent field terms to include these effects:

$$P - P' = aP + bQ + P_1 \quad (4)$$

$$Q - Q' = dP + eQ + Q_1 \quad (5)$$

$$Z - Z' = gP + hQ + R_1 \quad (6)$$

Denoting the average Z over the calibration areas by $\bar{Z}$, the constant terms can be expressed as:

$$P_1 = c\bar{Z} + P_0 \quad (7)$$

$$Q_1 = f\bar{Z} + Q_0 \quad (8)$$

$$R_1 = k\bar{Z} + R_0 \quad (9)$$

The error in Equations 4 to 6, of course, is the amount by which Z varies from $\bar{Z}$, multiplied by the appropriate coefficient c, f, or k.

Expressing P and Q in terms of the horizontal intensity H and the magnetic heading of the aircraft ψ, we have

$$P = H \cos \psi \quad (10)$$

$$Q = -H \sin \psi \quad (11)$$

Similarly, if H' is the apparent horizontal intensity and ψ' the apparent magnetic heading, we have:

$$P' = H' \cos \psi' \quad (12)$$

$$Q' = -H' \sin \psi' \quad (13)$$

The apparent components H' and D' are related to the measured component H* and D* through the constant calibration corrections h_o and d_o:

$$H' = H^* + h_o \quad (14)$$

$$D' = D^* + d_o \quad (15)$$

The constant calibration correction to Z* cannot be separated from R_0 and so it is arbitrarily taken as zero. The development of the calibration corrections was given by Haines and Hannaford (1976).

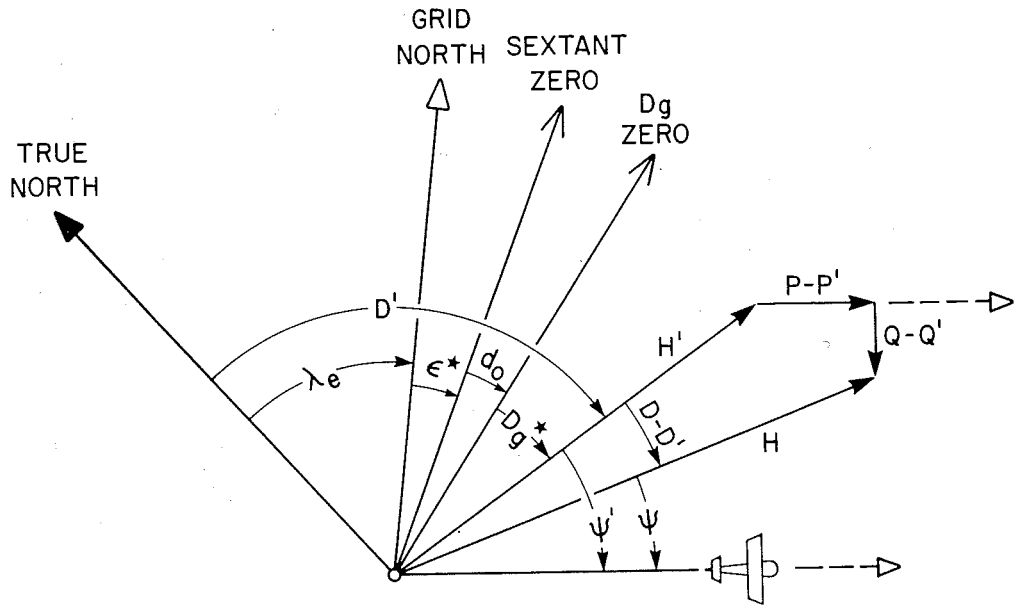

Figure 2. Horizontal fields and angles relevant to the determination of D and H.

The angle D* is not measured as a single quantity but is the sum of the east longitude λ_e, the observed angle D_g^*, and the observed deviation ε^* (see Figure 2):

$$D^* = \lambda_e + \varepsilon^* + D_g^* \qquad 16$$

The angle D_g^* is the measurement of the angle D_g' between apparent magnetic north and the gyro; the two may differ by a few tenths of a degree due to small constant errors in the digital voltmeter, precision voltage supply, or precision potentiometer. The angle ε^* is the measurement of the angle ε between grid north (the direction of true north plus east longitude) and the gyro, but again ε^* may differ from ε by a few tenths of a degree due to imprecise alignment when the sextant is initially mounted in the aircraft. The sum of these differences is the calibration correction angle d_o of Equation 15:

$$d_o = (\varepsilon - \varepsilon^*) + (D_g' - D_g^*) \qquad 17$$

The differences of course cannot be separated and so the gyro direction is not shown in the figure. In practice, the gyro is aligned before takeoff approximately in the direction of grid north. The sextant's horizontal circle zero is then aligned with the gyro and a servo maintains this alignment through the flight.

The deviation ε^* is determined by adding the grid azimuth (the azimuth relative to grid north) to the sextant horizontal circle reading (HCR) of the astronomical body being observed (see Figure 3):

$$\varepsilon^* = Az - \lambda_e + HCR \qquad 18$$

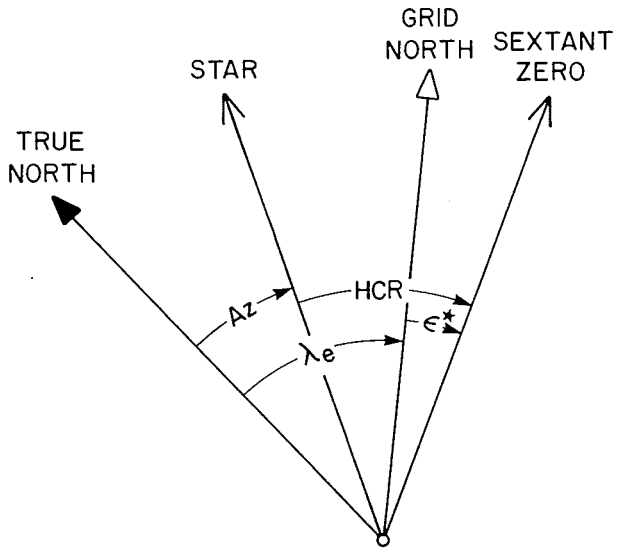

Figure 3. Determination of gyro deviation from sextant observation.

The true azimuth Az of the body (its azimuth relative to true north) is computed from the ephemeris values of astronomical declination and Greenwich hour angle, and the position of the aircraft at the time of observation. Sextant observations are made frequently throughout the flight, enabling a smooth curve to be drawn of ε^* versus time. Figure 4 shows the observed deviations and resulting smooth curve for part of Flight 13. On several flights the sextant was not precisely level and small corrections had to be applied to the observed HCR values.

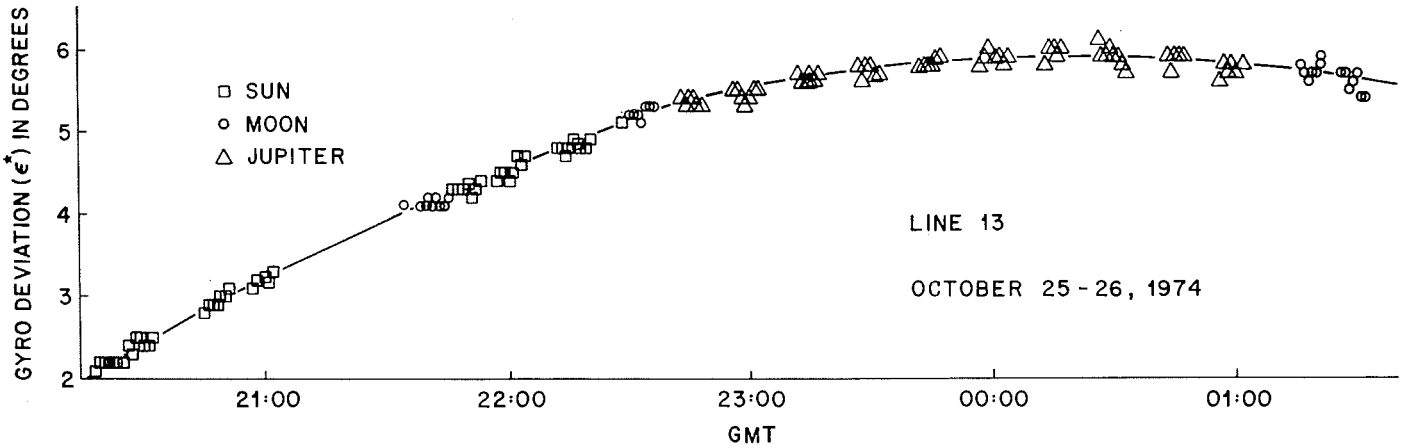

Figure 4. Plot of gyro deviations for part of Flight 13.

The apparent magnetic heading can be expressed as

$$\psi' = \psi + D - D' \qquad 19$$

$$= \psi + D - D^* - d_o \qquad 20$$

The horizontal corrections can then be written as

$$P - P' = H \cos \psi - (H^* + h_o) \cos (\psi + D - D^*) - d_o H^* \sin (\psi + D - D^*) + \{(1 - \cos d_o) H' \cos (\psi + D - D^*) + [(d_o - \sin d_o) H^* - h_o \sin d_o] \sin (\psi + D - D^*)\} \qquad 21$$

$$Q - Q' = -H \sin \psi + (H^* + h) \sin (\psi + D - D^*) - d_o H^* \cos (\psi + D - D^*) + \{-(1 - \cos d_o) H' \sin (\psi + D - D^*) + [(d_o - \sin d_o) H^* - h_o \sin d_o] \cos (\psi + D - D^*)\} \qquad 22$$

The terms in braces are generally small, for normal values of d_o and h_o. For example, if h_o = 100 nT, $d_o = 1^o$, and H^* = 16000 nT, the terms are less than 3 nT. Hence we may write:

$$P - P' = H \cos \psi - H^* \cos (\psi + D - D^*) - h_o \cos (\psi + D - D^*) - d_o H^* \sin (\psi + D - D^*) \qquad 23$$

$$Q - Q' = -H \sin \psi + H^* \sin (\psi + D - D^*) + h_o \sin (\psi + D - D^*) - d_o H^* \cos (\psi + D - D^*) \qquad 24$$

The calibration corrections and the induced and permanent aircraft field corrections can now be readily solved by the method of least-squares. The equations are:

$$H \cos \psi - H^* \cos (\psi + D - D^*) = h_o \cos (\psi + D - D^*) + d_o H^* \sin (\psi + D - D^*) + aH \cos \psi - bH \sin \psi + P_1 \qquad 25$$

$$-H \sin \psi + H^* \sin (\psi + D - D^*) = -h_o \sin (\psi + D - D^*) + d_o H^* \cos (\psi + D - D^*) + dH \cos \psi - eH \sin \psi + Q_1 \qquad 26$$

$$Z - Z' = gH \cos \psi - hH \sin \psi + R_1 \qquad 27$$

The aircraft-field correction to F can be derived from the component corrections. Using the 1st order bionomial approximation, we have

$$F - F' = \{(P - P') \cos \psi - (Q - Q') \sin \psi\} H/F + (Z - Z') Z/F \qquad 28$$

Expressing the component corrections by Equations 1 to 3 in terms of the permanent and induced correction parameters, and using Equations 10 and 11:

$$F - F' = \{a \cos^2 \psi - (b + d) \cos \psi \sin \psi + e \sin^2 \psi\} H^2/F + \{(c + g)Z + P_0\} (H/F) \cos \psi - \{(f + h)Z + Q_0\} (H/F) \sin \psi + \{kZ + R_0\} Z/F \qquad 29$$

Again, since Z varies so little over the calibration (or "swing") areas, we cannot distinguish between the Z-induced terms and the permanent terms:

$$F - F' = \{a \cos^2 \psi - (b + d) \cos \psi \sin \psi + e \sin^2 \psi\} H^2/F + P_2 (H/F) \cos \psi + Q_2 (H/F) \sin \psi + R_1 (Z/F) \qquad 30$$

where

$$P_2 = (c + g) \bar{Z} + P_0 \qquad 31$$

$$= g\bar{Z} + P_1 \qquad 32$$

$$Q_2 = (f + h) \bar{Z} + Q_0 \qquad 33$$

$$= h\bar{Z} + Q_1 \qquad 34$$

EFFECT OF MAGNETOMETER ORIENTATION

Suppose the magnetometer is not oriented precisely in the P', Q', Z', coordinate system, but instead in a P", Q", Z" system. If the direction cosines of the P" axis relative to the P', Q', Z' axes are a_1, a_2, a_3, those of Q" are b_1, b_2, b_3, and those of Z" are c_1, c_2, c_3, the equations of coordinate rotation from the P', Q', Z' system to the P", Q", Z" system are

$$P'' = a_1P' + a_2Q' + a_3Z' \quad (35)$$

$$Q'' = b_1P' + b_2Q' + b_3Z' \quad (36)$$

$$Z'' = c_1P' + c_2Q' + c_3Z' \quad (37)$$

Of course, there are six orthogonality constraints on the direction cosines, so that any three of the cosines can be expressed in terms of the other six.

Substituting the values of P', Q', Z' from Equations 1 to 3 we get the corrections due to both aircraft-fields and magnetometer orientation:

$$\begin{aligned} P-P'' = {} & [1 - a_1(1-a) + a_2d + a_3g]\ P \\ & + [a_1b - a_2(1-e) + a_3h]\ Q \\ & + [a_1c + a_2f - a_3(1-k)]\ Z \\ & + [a_1P_0 + a_2Q_0 + a_3R_0] \end{aligned} \quad (38)$$

$$\begin{aligned} Q-Q'' = {} & [-b_1(1-a) + b_2d + b_3g]\ P \\ & + [1 + b_1b - b_2(1-e) + b_3h]\ Q \\ & + [b_1c + b_2f - b_3(1-k)]\ Z \\ & + [b_1P_0 + b_2Q_0 + b_3R_0] \end{aligned} \quad (39)$$

$$\begin{aligned} Z-Z'' = {} & [-c_1(1-a) + c_2d + c_3g]\ P \\ & + [c_1b - c_2(1-e) + c_3h]\ Q \\ & + [c_1c + c_2f - c_3(1-k)]\ Z \\ & + [c_1P_0 + c_2Q_0 + c_3R_0] \end{aligned} \quad (40)$$

The equations have exactly the same form as Equations 1 to 3. That is, we can consider that the correction parameters a, b, c,..., P_0, Q_0, R_0 in Equations 1 to 3 (or a, b, d,..., P_1, Q_1, R_1 in Equations 4 to 6) include both the effects of aircraft fields and of magnetometer orientation. Indeed, the two effects cannot be separated: the one is indistinguishable from the other.

We can express the coefficients in terms of rotation angles, and include the effects of the orthogonality constraints, by considering the first-order approximation to the above equations. We express the (small) orientation angles in terms of the angles of rotation about the P', Q' and Z' axes, respectively called roll (r), pitch (p) and yaw(y). Roll and pitch will be considered positive downwards, and yaw positive to the right. In terms of the direction cosines, we have approximately: arc cos $a_2 = \pi/2 - y$; arc cos $a_3 = \pi/2 - p$; arc cos $b_3 = \pi/2 - r$. The corrections become:

$$P - P'' = a\ P + (b-y)\ Q + (c-p)\ Z + P_0 \quad (41)$$

$$Q - Q'' = (d+y)\ P + e\ Q + (f-r)\ Z + Q_0 \quad (42)$$

$$Z - Z'' = (g+p)\ P + (h+r)\ Q + k\ Z + R_0 \quad (43)$$

As before, if the Z - variation is insufficient for the statistically significant determination of the Z coefficients, we have

$$P - P'' = a\ P + (b-y)\ Q + P_1 \quad (44)$$

$$Q - Q'' = (d+y)\ P + e\ Q + Q_1 \quad (45)$$

$$Z - Z'' = (g+p)\ P + (h+r)\ Q + R_1 \quad (46)$$

where

$$P_1 = (c-p)\ \overline{Z} + P_0 \quad (47)$$

$$Q_1 = (f-r)\ \overline{Z} + Q_0 \quad (48)$$

$$R_1 = k\ \overline{Z} + R_0 \quad (49)$$

The F-corrections, Equations 29 and 30, remain unchanged.

It is emphasized again that the orientation corrections are indistinguishable from the induced-field corrections. They are separated here merely to indicate an alternative interpretation to some of the coefficients. The most general form of the corrections is Equations 1 to 3, which include both aircraft-field and orientation corrections.

SWING-DERIVED CORRECTIONS

The method of swing-derived corrections has been explained in detail by Haines and Hannaford (1976).

During this survey, three swing flights were made over Rosaire, Quebec: one of 13 passes and another of 10 at the beginning of the survey and one of 10 passes at the end. Three partial swings of 4, 6, and 2 passes were made in the middle of the survey over Resolute Bay, District of Franklin.

The swing-derived corrections for the two magnetometer systems (the least-squares solutions of Equations 25 to 27 and Equation 30), with standard errors affixed as $\pm$ quantities, are as follows:

Fluxgate Magnetometer

$d_o = .76 \pm .08^o$

$a = -.0063 \pm .0018$

$P_1 = 165 \pm 18$ nT

$Q_1 = -284 \pm 18$ nT

$g = -.0026 \pm .0005$

$R_1 = 150$ nT

Proton Magnetometer

$a = -.0100 \pm .0005$

$e = -.0081 \pm .0006$

$Q_2 = -12 \pm 7$ nT

$R_1 = 9.8 \pm 1.5$ nT

The parameters h_o, b, d, and e for the fluxgate magnetometer and (b+d) and P_2 for the proton magnetometer were found to be statistically not significant, and were taken to be zero.

It was shown in the previous section that the g parameter can be interpreted as the sum of an induced coefficient and an orientation (pitch) error: $g = g_{ind} + p$, say. It is quite feasible that the derived value of -.0026, for the fluxgate magnetometer, is due entirely to a pich error (of $-.15^o$). This interpretation would explain why this type of variation exists on one survey but is not evident on others. Furthermore, it suggests that the permanent part of the aircraft-field (P_0) is almost entirely transverse since, from Equation 47 and the above expression for g, $P_0 = P_1 - (c_{ind} + g_{ind} - g)\,\bar{Z} = 17$ nT when the induced coefficients c_{ind} and g_{ind} are both zero. One would expect the permanent field at the fluxgate sensors to be transverse if it is mainly due to electrical currents, since they travel along a cable above the ceiling and return along the fuselage. In fact, the mean phase of the aircraft field corrections over the last four EPB surveys was -89 ± 12^o.

The swing values H - H' and H(D-D') are plotted against magnetic heading ψ in Figure 5. Since the corrections depend on H, adjustments were made to the Resolute Bay values so that they could be put on the same plot as the Rosaire values. The least-squares correction curves, for H = 15775 nT (the mean value at Rosaire), are also shown.

The vertical aircraft-field correction R_1 changed significantly from one swing flight to another. This was observed previously in the EPB aeromagnetic survey of 1972 (Haines and Hannaford, 1976, Figures 3 and 6).

In solving for g and h (Equation 27) it was assumed that R_1 was constant over each swing. The resulting "swing-constant" R_1 were as follows:

FLIGHT	R_1	ST. ERROR
3	54	9 nT
7	98	10
17	201	16
19	118	14
20	179	22
32	166	10

Figure 6 shows Z - Z' corrected for these swing-constant R , for the Rosaire swings (Flights 3, 7 and 32) and for the Resolute Bay swings (Flights 17, 19 and 20). The least-squares correction curve is also shown for the respective values of H (15775 nT at Rosaire, 775 nT at Resolute Bay). The difference in scatter between the two curves represents the difference in the effect of platform tilt at the two locations. A 6' error in the vertical results in a 27 nT error in Z at Rosaire, but only 1 nT at Resolute Bay.

The given "swing-derived" value of 150 nT for R_1 comes not from taking a simple mean or weighted mean, but from plotting the swing-constant R_1 versus time and estimating the survey mean from the resulting curve. It will be seen later that the "consistency-derived" Z-correction cancels out any error in the swing-derived R_1.

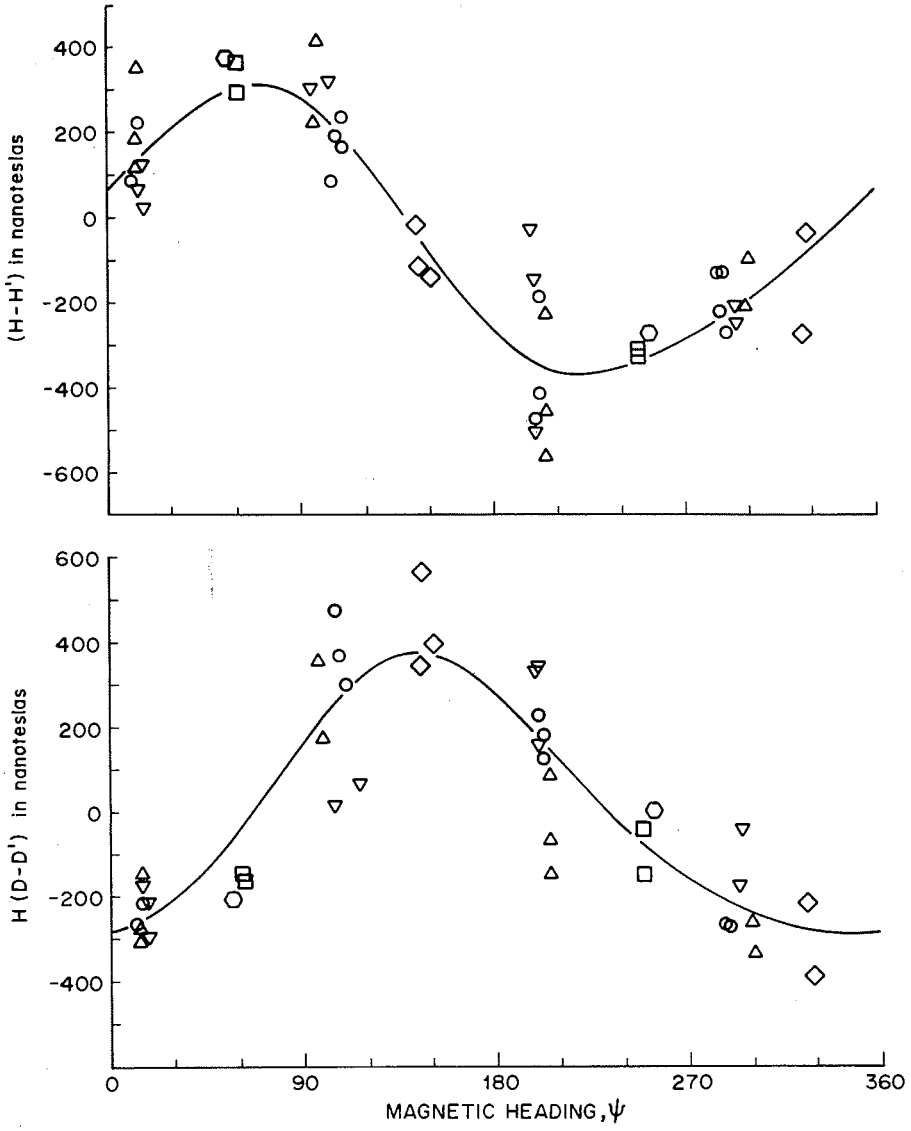

Figure 5.

Swing-derived corrections to fluxgate-measured D and H. Circles, up-pointing triangles, and down-pointing triangles apply to Rosaire swing flights 3, 7 and 32, respectively; squares, diamonds, and hexagons apply to Resolute Bay partial-swing flights 17, 19 and 20, respectively. Adjustments were made to the Resolute Bay values for comparison with swing-derived correction curve for Rosaire (H=15755 nT).

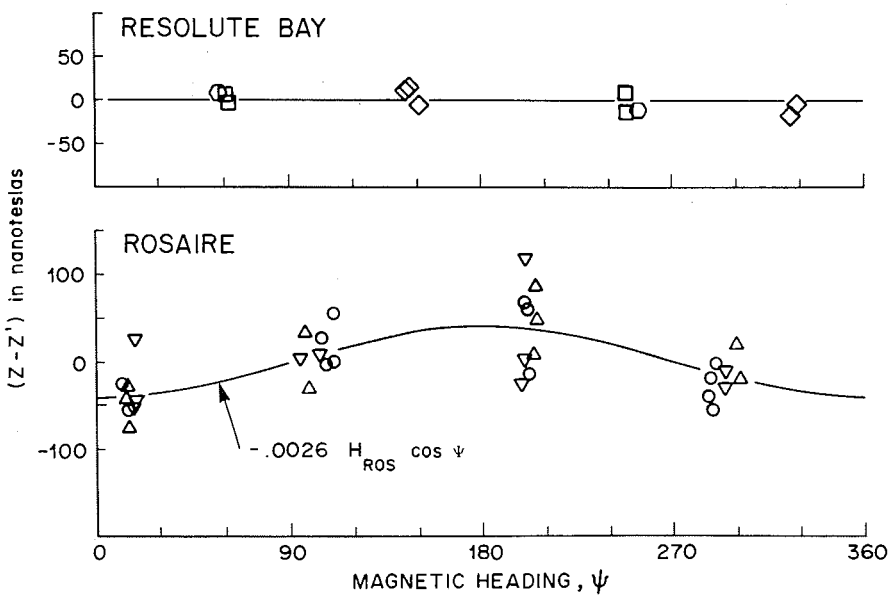

Figure 6.

Swing-derived corrections to fluxgate-measured Z, after removal of "swing-constant" values for R_1, for Rosaire swings and for Resolute Bay swings. Symbols are same as in Figure 5. Correction curves are shown for H=15775 nT at Rosaire and for H=775 nT at Resolute Bay.

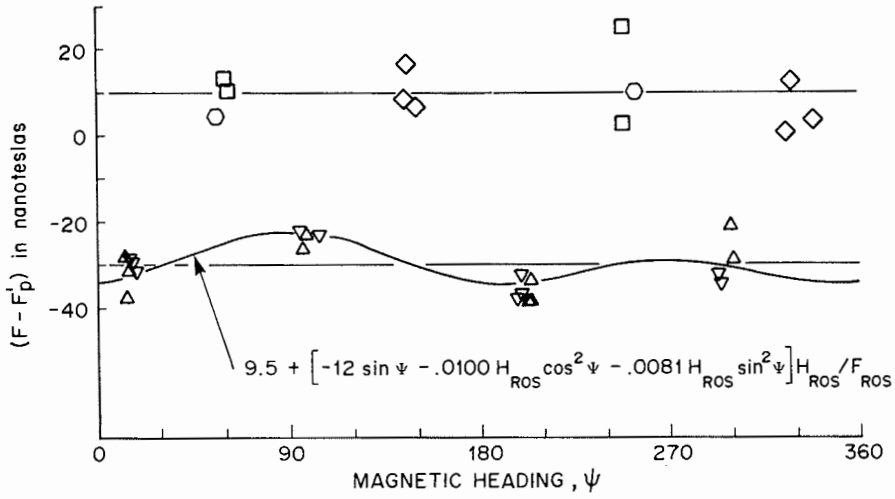

Figure 7.

Swing-derived corrections to proton-measured F. Symbols are same as in Figure 5. Correction curves are shown for H=15775 nT at Rosaire and for H=775 nT at Resolute Bay.

The F-F' values for the proton magnetometer are shown in Figure 7. Unfortunately, the proton magnetometer was not working during the first Rosaire swing (Flight 3). Shown also on the plot is the least-squares correction curve for Resolute Bay and for Rosaire. There is a mean level difference between both curves, absorbed here by the $\cos^2 + \sin^2$ effect of the parameters a and e. Mean level differences of 26 and 21 nT were observed on two previous (1970 and 1972) surveys, between Meanook and Rosaire. These were considered to be due to differences in processing ground information (Haines and Hannaford, 1976). A further level difference of 7 nT on the 1970 survey, between Resolute Bay and Meanook, was not considered at the time to be significant. It is felt now, however, that the differences in methods of processing cannot explain level differences of the magnitudes observed, and the consistency of results over three surveys led to the adoption of induced fields as an explanation for these level differences.

CORRECTION OF DATA

A previous section dealt with the solution of calibration, aircraft-field, and orientation correction parameters, given the true values of D, H, Z and F, the true magnetic heading ψ, and the measured values D*, H*, Z* and F*. Here we derive values of D, H, Z, and F from the apparent magnetic heading ψ' and the measured values D*, H*, Z* and F*, given the correction parameters d_o, h_o, a, b, etc.

The solution of Equations 4 and 5 yields

$$P = \frac{1}{1-a}(P'+P_1) + \frac{b}{(1-a)(1-e)-bd}(Q'+Q_1) \quad 50$$

$$Q = \frac{1}{1-e}(Q'+Q_1) + \frac{d}{(1-a)(1-e)-bd}(P'+P_1) \quad 51$$

However, if the magnitudes of the correction parameters are small, and the required accuracy for P and Q not too great, the first-order solution will be sufficient:

$$P = (1+a)\,P' + bQ' + (1+a)\,P_1 + bQ_1 \quad 52$$

$$Q = dP' + (1+e)\,Q' + dP_1 + (1+e)\,Q_1 \quad 53$$

For this survey, for example, the error in this first-order solution is less than 0.7 nT. In fact, the errors in the least-squares determination of the correction parameters result in a much larger error than this and do not warrant any higher degree of accuracy.

Expressing P' and Q' in terms of H* and ψ':

$$P = (H^* + h_o)\,[(1+a)\cos\psi' - b\sin\psi'] + (1+a)\,P_1 + bQ_1 \quad 54$$

$$Q = (H^* + h_o)\,[d\cos\psi' - (1+e)\sin\psi'] + dP_1 + (1+e)\,Q_1 \quad 55$$

The corrected values ψ, H, and D are then given by:

$$\psi = \arctan(-Q/P) \qquad 56$$

$$H = \sqrt{P^2 + Q^2} \qquad 57$$

$$D = (D^* + d_o) + \psi' - \psi \qquad 58$$

where the arctangent must be taken in the quadrant appropriate to the signs of P and Q.

Having ψ and H, we can use Equation 27 directly to obtain Z.

To use Equation 30 for determining the correction F - F' at the proton magnetometer, we use ψ, H, and Z as determined in Equations 56, 57, and 27. Furthermore, since Z/F is essentially constant over the survey area, $R_1(Z/F)$ was taken as a constant, 9.5 nT.

If there is no D* from which to derive a magnetic heading ψ, the apparent magnetic heading ψ' is used in Equations 27 and 30 to derive Z and F. Additionally, if there is no H*, and hence no H, we compute H from the International Geomagnetic Reference Field for the purpose. Since the induced component of the Z and F corrections are small, the error caused by these substitutions amount only to a few nanoteslas. In the majority of cases, however, D*, H*, Z* and F* are all available.

CONSISTENCY-DERIVED CORRECTIONS FOR Z

Over the survey area, Z is close to F and so the proton magnetometer, which is housed outside the aircraft and hence not sensitive to aircraft-fields, can be used to determine the variation in the vertical aircraft-field correction at the fluxgate magnetometer inside the aircraft. This variation, so derived, is termed the "consistency-derived correction" for Z. The method of obtaining consistency-derived corrections was explained by Haines and Hannaford (1976).

The basic expression is:

$$\delta R = (F/Z)\left\{(F_p - F_f) - \delta P(H/F)\cos\psi + \delta Q(H/F)\sin\psi\right\} \qquad 59$$

where δP and δQ are the (unknown) variations in the horizontal P and Q fields, and of course $F = \sqrt{H^2 + Z^2}$. This expression results from Equation 28 by putting $F = F_p$ and $F' = F_f$, where F_p and F_f have been corrected on the basis of their respective swing-derived corrections.

The overall Z-correction (Equation 27) then becomes:

$$Z - Z' = gH\cos\psi - hH\sin\psi + R_1 + \delta R \qquad 60$$

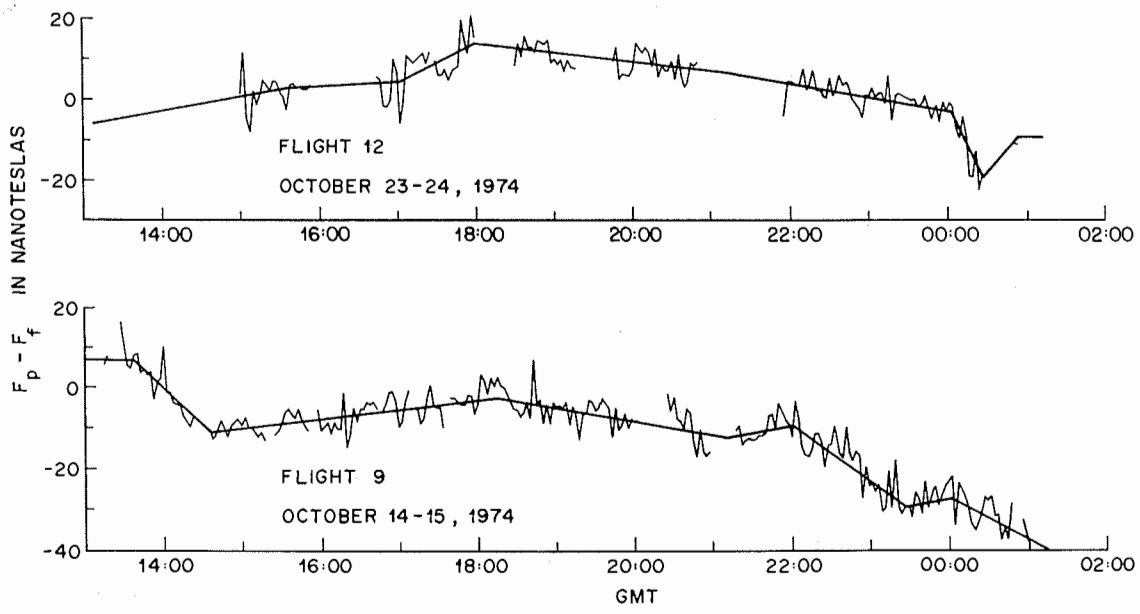

Figure 8. Plots of $F_p - F_f$ versus time for Flights 9 and 12. The linear line-segments were visually chosen and are the "consistency-derived" time-varying Z-corrections.

For the EPB 1972 survey the effects of δP and δQ were removed by averaging $F_p - F_f$ over each flight, since most of the flights comprised lines flown on headings 180° apart. Thus the Z correction was different for each flight, but was constant within the flight itself. This resulted in a 19 nT scatter of the final $F_p - Ff$ values over the survey.

For this survey we have attempted to correct for the within-flight variation as well. Figure 8, for example, shows a plot of how $F_p - F_f$ varies with time over Flights 9 and 12.

Linear line-segments were fitted visually to the plots of $F_p - F_f$ versus time, as in Figure 8. The result for all flights is shown in figure 9. There is a steady increase from flight to flight over the first half of the survey, but the trend in the second half is not as definite as that in the first. The scatter of the $F_p - F_f$ values about the line-segments for the entire survey is 4 nT.

Figure 9 demonstrates how the F_f correction field changes with time over the survey. The method is independent of diurnal or disturbance fields, since both F_p and Ff will be affected in the same way. Similarly it is independent of platform or magnetometer orientation, since F_f is the magnitude of the total magnetic vector at the fluxgate. An analysis of plots similar to those in Figure 8 showed that there was little heading effect compared to the overall field variations. This is probably due to the H/F factor (see Equation 59) which for most of the survey was very small. Hence, we ignore the terms involving δP and δQ and treat the $F_p - F_f$ variation as resulting only from the δR variation in the vertical Z field. Furthermore, the F/Z factor can be ignored with very little error (generally 1 or 2 nT, and certainly less than the error resulting from putting $\delta P = \delta Q = 0$).

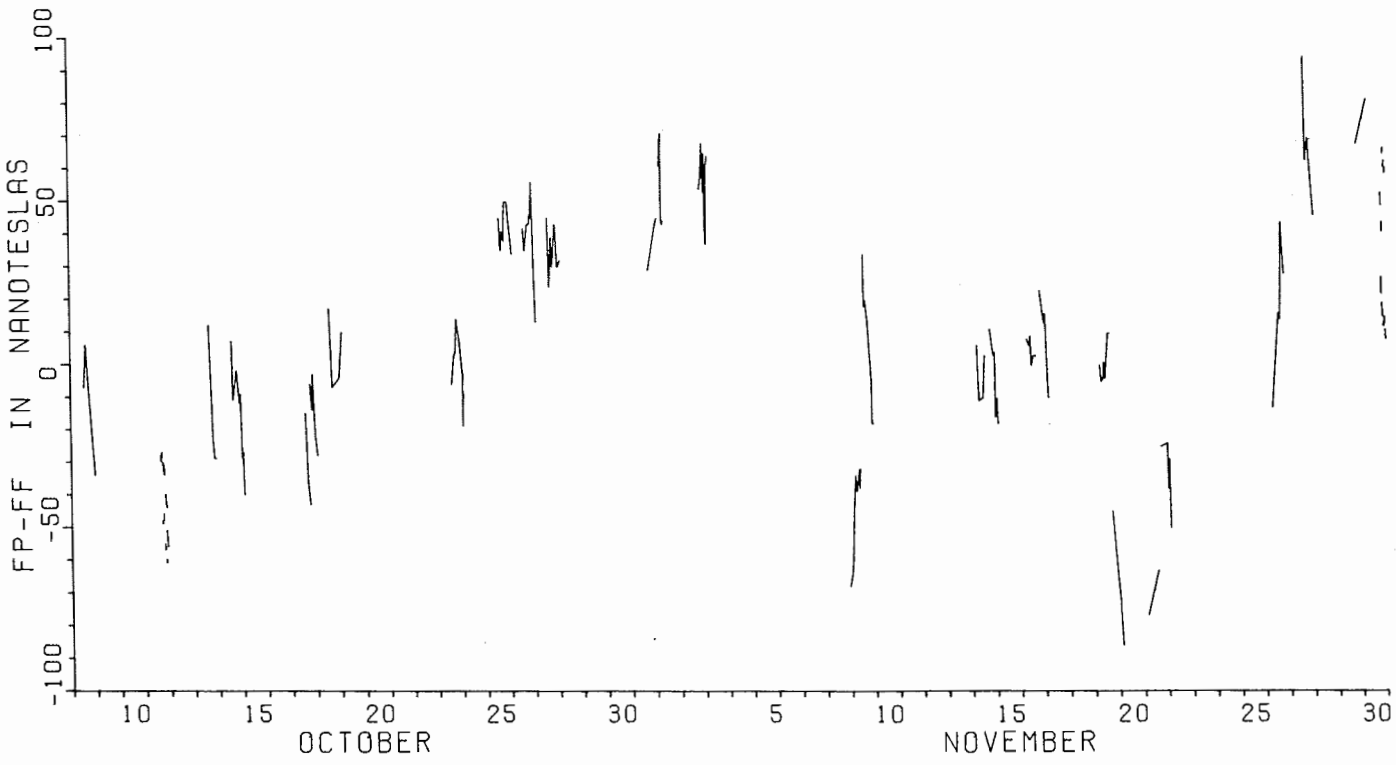

Figure 9. Plot of F_p-Ff line-segments for 1974 aeromagnetic survey. These time-varying line-segments were taken as the consistency-derived corrections for Z.

The linear line-segments of $F_p - F_f$ (Figure 9) are thus taken as the consistency-derived time-varying Z correction δR.

It will be noted that any "error" in the swing-derived R_1 will be cancelled by the δR. Increasing the R_1 will decrease the resulting δR by an equal amount.

In computing the (swing-derived) g and h of Equation 27, the R_1 was taken to be constant over each swing. This can be checked with how the δR varies over each swing. If necessary, g and h could be re-computed; for this survey, however, the δR were constant within a few nanoteslas and no recalculation was considered necessary.

The survey Z-data are finally recorrected (by Equation 60) on the basis of the new consistency-derived time-dependent correction δR.

DATA REJECTION FOR MAGNETIC DISTURBANCE

There are six magnetic observatories close to the survey area: Ottawa, Great Whale River, Churchill, Baker Lake, Cambridge Bay, and Resolute Bay. Values of X,Y, and Z at 1-minute intervals are available for each of these observatories. The aeromagnetic data and the observatory data for the same time intervals were transformed to the cylindrical coordinates H, DH, and Z, and plotted versus time at 250 nT/inch versus 1 hour/inch.

Since a magnetic disturbance at any given time will be confined to a certain range of magnetic latitudes, the position of the aircraft must be considered in determining whether or not the field at the aircraft is affected by the disturbance. Then by visual inspection of the aeromagnetic and relevant observatory data plots, a decision is made whether to accept or reject the survey data. For this decision, Z was considered separately from D and H. That is, Z was accepted for some intervals during which D and H were rejected.

The criterion used for data acceptance was that the fields at the relevant observatories lie within a 100 nT band over a time interval of 3 hours or more. No diurnal or disturbance corrections were made to these data. They were merely accepted as measured, and are accurate in this respect only to the extent of the validity and accuracy of the acceptance method.

Unfortunately, a very large proportion (38%) of the data were considered to be disturbed and were rejected. We are studying the possibility of correcting these data for disturbance fields, although some of the observed disturbances are of such magnitude and complexity that a meaningful correction will be impossible to determine. This is the case for about 3/4 of the rejected data. In other words, of the total 1974 survey data, 62% are considered "relatively undisturbed", 11% are disturbed but may be correctable by ionospheric current modelling or some other method, and 27% are very disturbed and considered not correctable.

The accepted ("relatively undisturbed") aeromagnetic data are believed to be comparable to those of previous EPB surveys, with respect to diurnal variation and minor disturbance-field content.

PRESENTATION OF DATA

Haines and Hannaford (1976) described the recording of 3-second raw data, the process of editing and massaging it, the forming and statistical editing by computer of 1/2-minute averages, the merging of any 1/2-minute averages that have to be derived manually, and finally the correction of these 1/2-minute averages for instrumental errors and aircraft fields.

They also described the method of reducing the data to sea level by the "inverse-cube relationship", and fitting a polynomial in two spatial coordinates to each of three orthogonal components U, V and Z. The horizontal components U and V are defined by:

$$U = H \cos [\, D - (\lambda - \lambda_o) \,] \qquad 61$$

$$V = H \sin [\, D - (\lambda - \lambda_o) \,] \qquad 62$$

where λ is the geographic east longitude and λ_o is a map rotation angle, chosen for this survey to be -180^o.

All polynomial coefficients determined by least-squares may not be statistically significant. That is, certain subsets of them may explain as well, or better, the variations observed in the data, since the insignificant terms may introduce noise and distort the true field. Choosing which subset is the best can be done by comparing contour plots of the polynomial minus a reference field with plots of residuals relative to the same reference field. Similar plots over adjacent survey areas can also be used as an indication of the field behaviour.

The standard errors of estimate of least-squares fits to 1st, 2nd, 3rd, and 4th degree polynomials, and to the adopted 3rd degree polynomials with significant terms only, are given in Table I.

Coefficients for the adopted 3rd degree polynomials are given in Table II. Definitions of the spatial coordinates and of the components U, V, and Z, as well as formulae relating U and V to the more familiar D, H, X, and Y, are also given in the Table.

A comparison of the International Geomagnetic Reference Field (IGRF) with the 3rd degree polynomial field of Table II is given in Figure 10. There are large biases in the IGRF over the area, as there are over areas of previous surveys (Haines and Hannaford, 1972, 1974, and 1976).

Profile plots of 1/2-minute IGRF residuals in D, H, Z, X, Y, and F are shown in Figures 11 to 16. A residual is a 1/2-minute average (corrected for instrumental errors, magnetometer orientation, and aircraft fields) minus the corresponding IGRF value for 1974.85 at the altitude of observation. The residuals, represented by the short lines joining the profile to the flight track, are plotted normal to the track, positive residuals being plotted in the right half-plane, negative in the left. Because of the scale reduction required for page-size publication, however, only every second residual was joined to the track.

The plots were produced entirely by computer, on a scale of 1:5,000,000. The coastline data-set is not accurate (in some places it is out by 35 km) and so anomalies should be located by using the latitude-longitude grid rather than the coastline.

TABLE I

Standard deviations in nanoteslas of observed minus polynomial fields of 1st, 2nd, 3rd, and 4th degree, and the adopted 3rd-degree with significant terms only (denoted by 3 sig). Coefficients column gives total number of coefficients in the three polynomials. Sample size = 1085 for U and V, 1533 for Z (every tenth 30 second average)

Degree	Coefficients	U	V	Z
1	9	268.1	641.6	1076.0
2	18	141.0	302.6	250.4
3	30	135.8	242.9	169.0
4	45	134.9	240.8	159.8
3 sig	23	136.3	243.4	169.0

TABLE II

3rd degree polynomial reference field in nanoteslas for 1974.85, at sea level.

$U = \Sigma u_i x_i \qquad V = \Sigma v_i x_i \qquad Z = \Sigma z_i x_i$

$a = -K \tan(\theta/2) \cos(\lambda - \lambda_o) - a_o$
$b = K \tan(\theta/2) \sin(\lambda - \lambda_o) - b_o$

θ = colatitude
λ = east longitude
K = 100.
λ_o = -180^o
a_o = 2.80
b_o = 26.65

$D = \arctan(V/U) + (\lambda - \lambda_o)$
$H = (U^2 + V^2)^{\frac{1}{2}}$
$X = U \cos(\lambda - \lambda_o) - V \sin(\lambda - \lambda_o)$
$Y = U \sin(\lambda - \lambda_o) + V \cos(\lambda - \lambda_o)$

i	x_i	u_i	v_i	z_i
1	1	-2818.32	-6188.34	60534.58
2	a	-743.862	70.552	-204.380
3	b	54.956	-616.692	51.782
4	a^2	4.3437		-17.1246
5	ab	-6.4789	3.1539	5.6281
6	b^2	1.6738	-8.4040	-16.3213
7	a^3			
8	a^2b	-.13647		-.20557
9	ab^2	.20380		.37910
10	b^3		.32068	-.31362

Note: Coefficients that were statistically insignificant are left blank, and are taken as zero.

ACKNOWLEDGMENTS

The authors wish to thank Conair Aviation Ltd. for their cooperation and in particular to thank Captains D. Maclagan, A. Melhof, and R. Nelson and Navigators A. Lyon and M. Mole for their help in conducting the survey.

The airborne scientific crew comprised Earth Physics Branch personnel F. Andersen, G. Carr, R. Charbonneau, and W. Hannaford. A ground station was set up and operated at the beginning of the survey by R. Groulx and G. Massie.

E.I. Loomer and G. Jansen van Beek provided Ottawa Observatory values for ground value control for the Rosaire swings, and ground values for the Resolute Bay swings. They also provided data tapes for the six observatories used in checking for magnetic disturbances.

R.L. Coles assisted in the determination of the magnetically disturbed time intervals for purposes of data rejection.

The authors wish to thank Dr. R.L. Coles and Dr. P.H. Serson for critically reviewing the manuscript and offering many helpful suggestions.

REFERENCES

Bowditch, N., 1962. American Practical Navigator, United States Navy Hydrographic Office, H. O. Pub. No. 9, U.S. Govt. Printing Office, Washington.

Haines, G.V. and W. Hannaford, 1972. Magnetic anomaly maps of British Columbia and the adjacent Pacific Ocean. Pub. Earth Phys. Br., Vol. 42, No. 7, pp. 211-228.

Haines, G.V. and W. Hannaford, 1974. A three-component aeromagnetic survey of the Canadian Arctic. Pub. Earth Phys. Br., Vol. 44, No. 8, pp. 209-234.

Haines, G.V. and W. Hannaford, 1976. A three-component aeromagnetic survey of Saskatchewan, Alberta, Yukon and the District of Mackenzie. Geomagnetic Service of Canada, Geomag. Series No. 8.

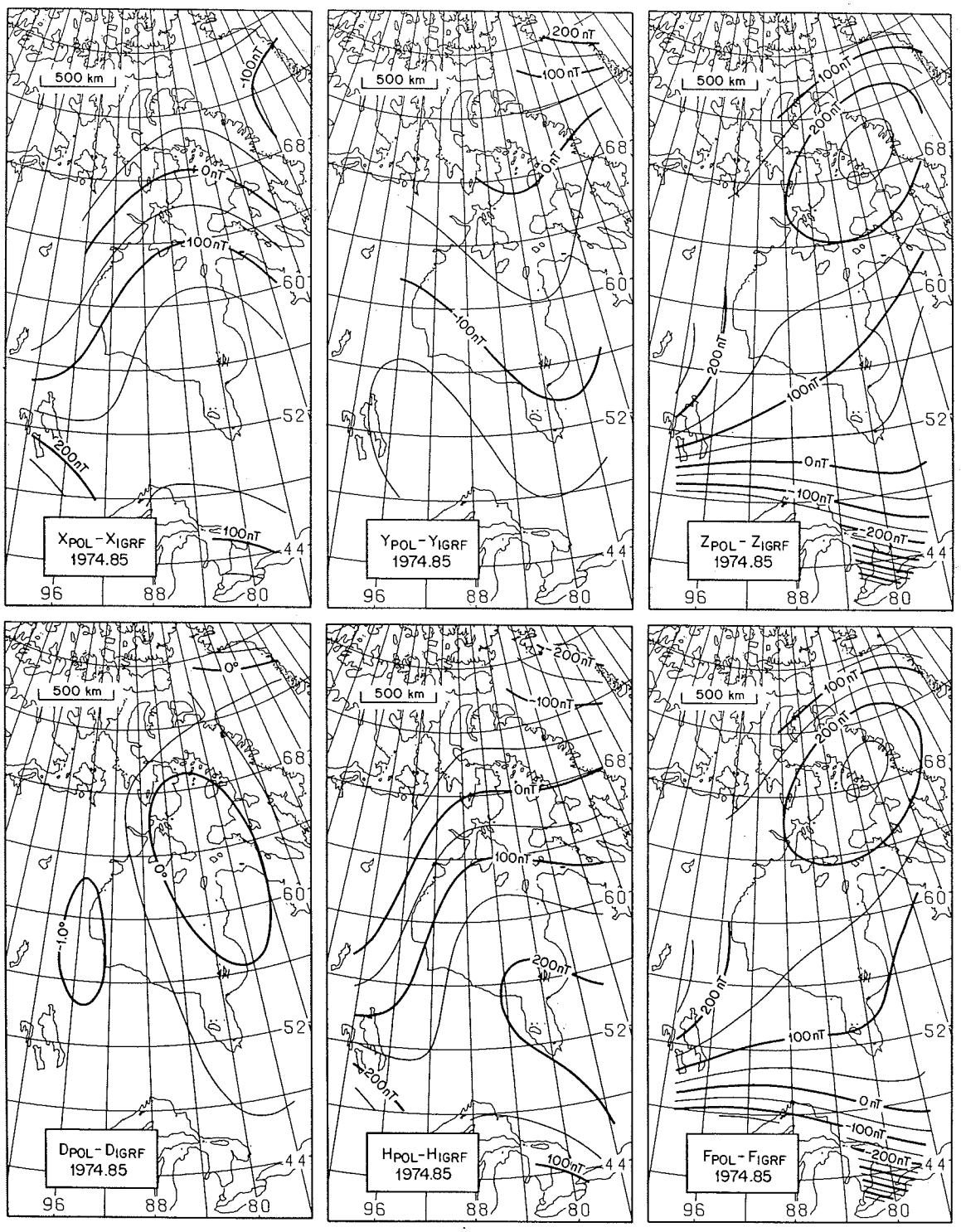

Figure 10. Comparison of International Geomagnetic Reference Field (IGRF) with 3rd degree polynomial (POL).

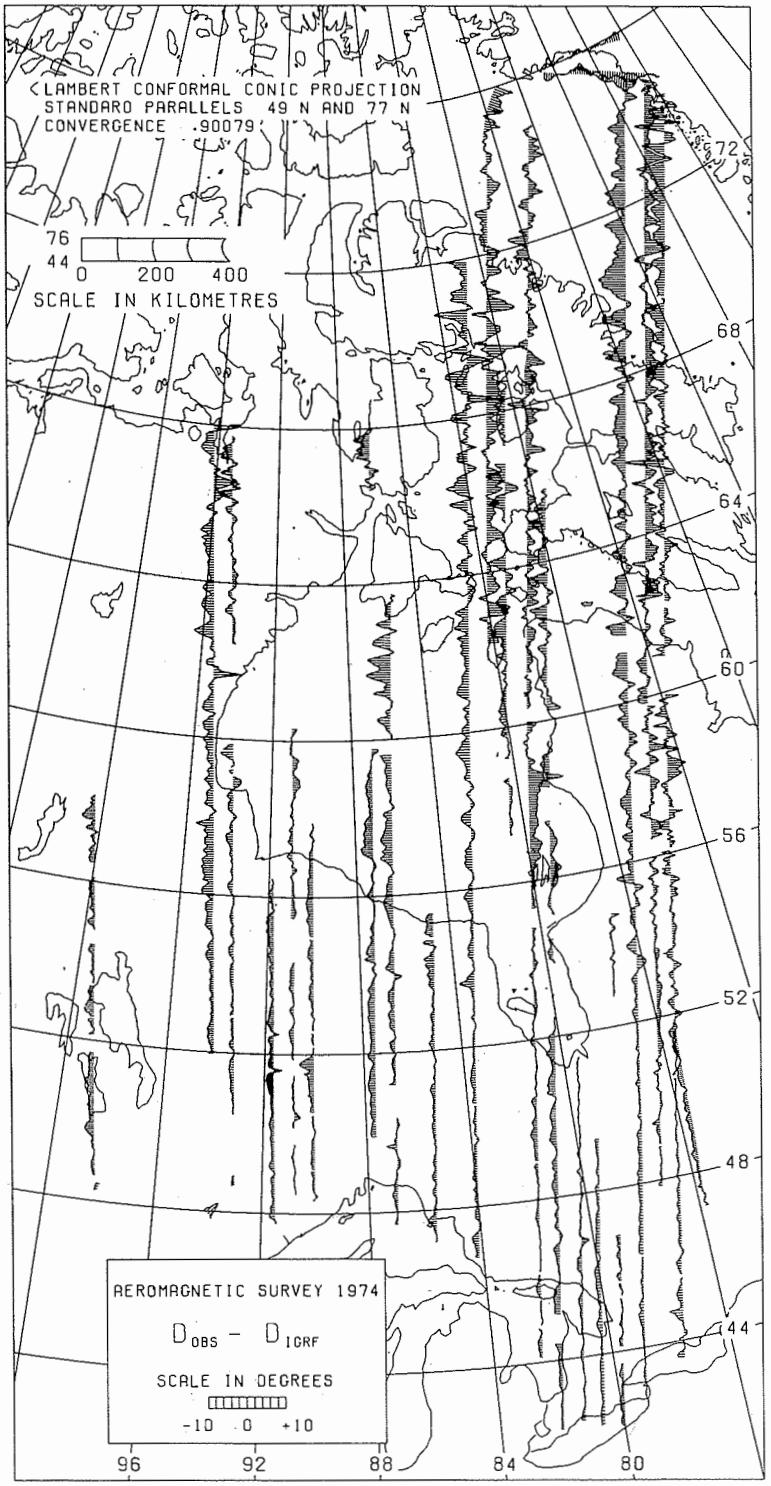

Figure 11. Residual profiles of declination D, relative to the International Geomagnetic Reference Field (IGRF), 1974.85. The residuals are 1/2-minute averages (corrected for instrumental errors, magnetometer orientation, and aircraft fields) minus the corresponding IGRF values for 1974.85 at the altitude of observation. Residuals are plotted normal to the flight track, positive residuals in the right half-plane, negative in the left. Only every second residual is joined to the flight track. The residual profile plots were produced entirely by computer, and the coastline is inaccurate in some places. Hence anomalies should be located by referring to the latitude-longitude grid.

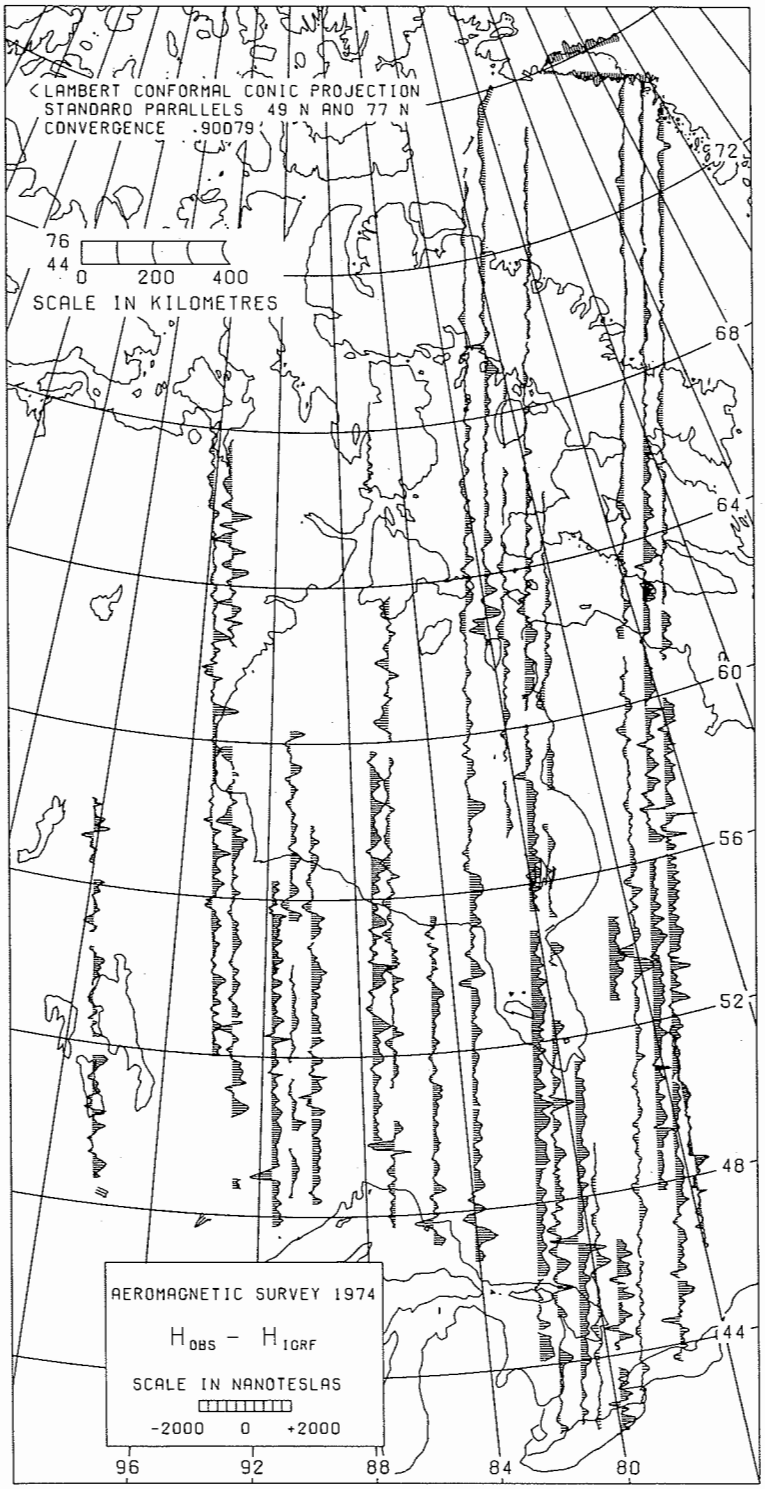

Figure 12. Residual profiles of horizontal intensity H, relative to the IGRF, 1974.85.

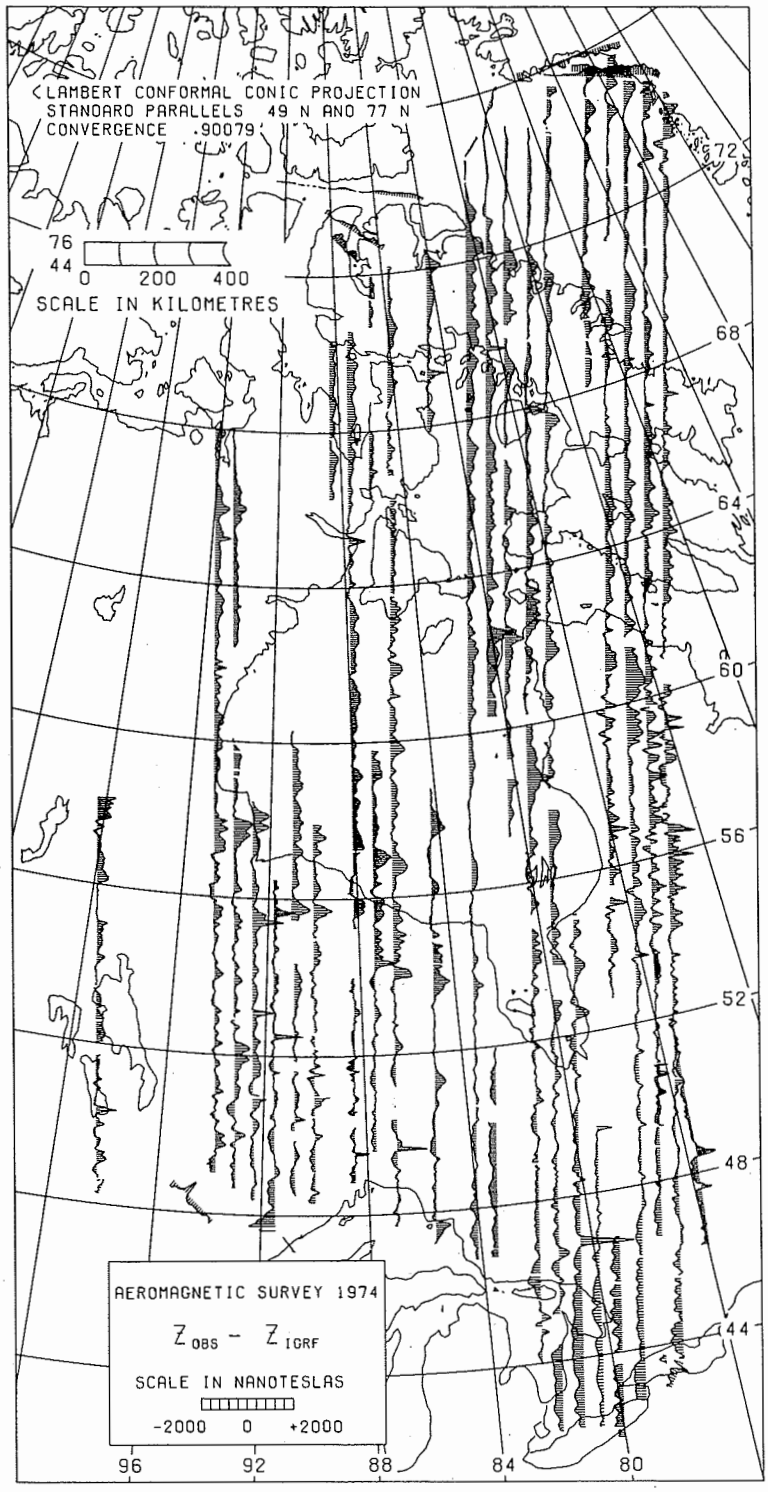

Figure 13. Residual profiles of vertical intensity Z, relative to the IGRF, 1974.85.

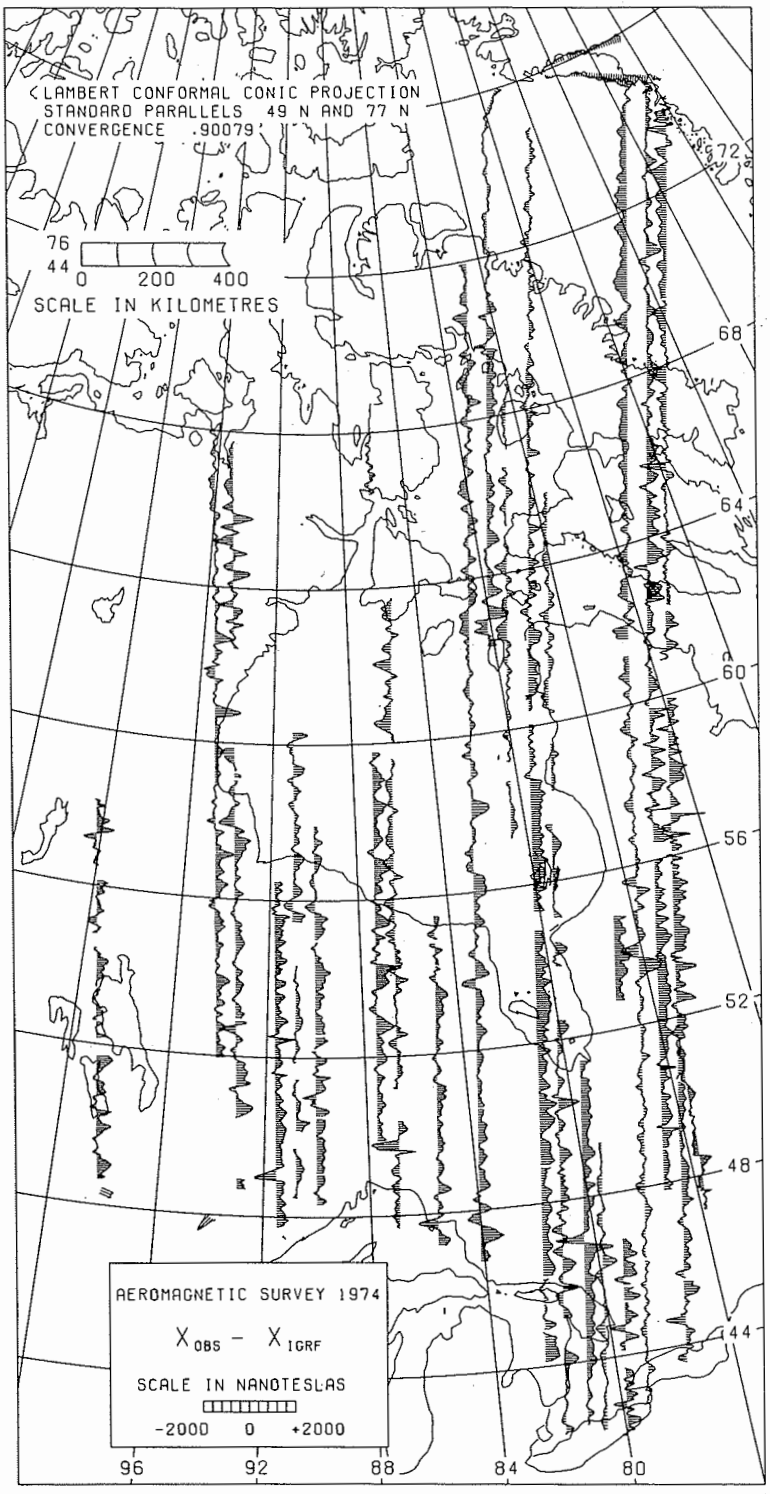

Figure 14. Residual profiles of geographic north component X, relative to the IGRF, 1974.85.

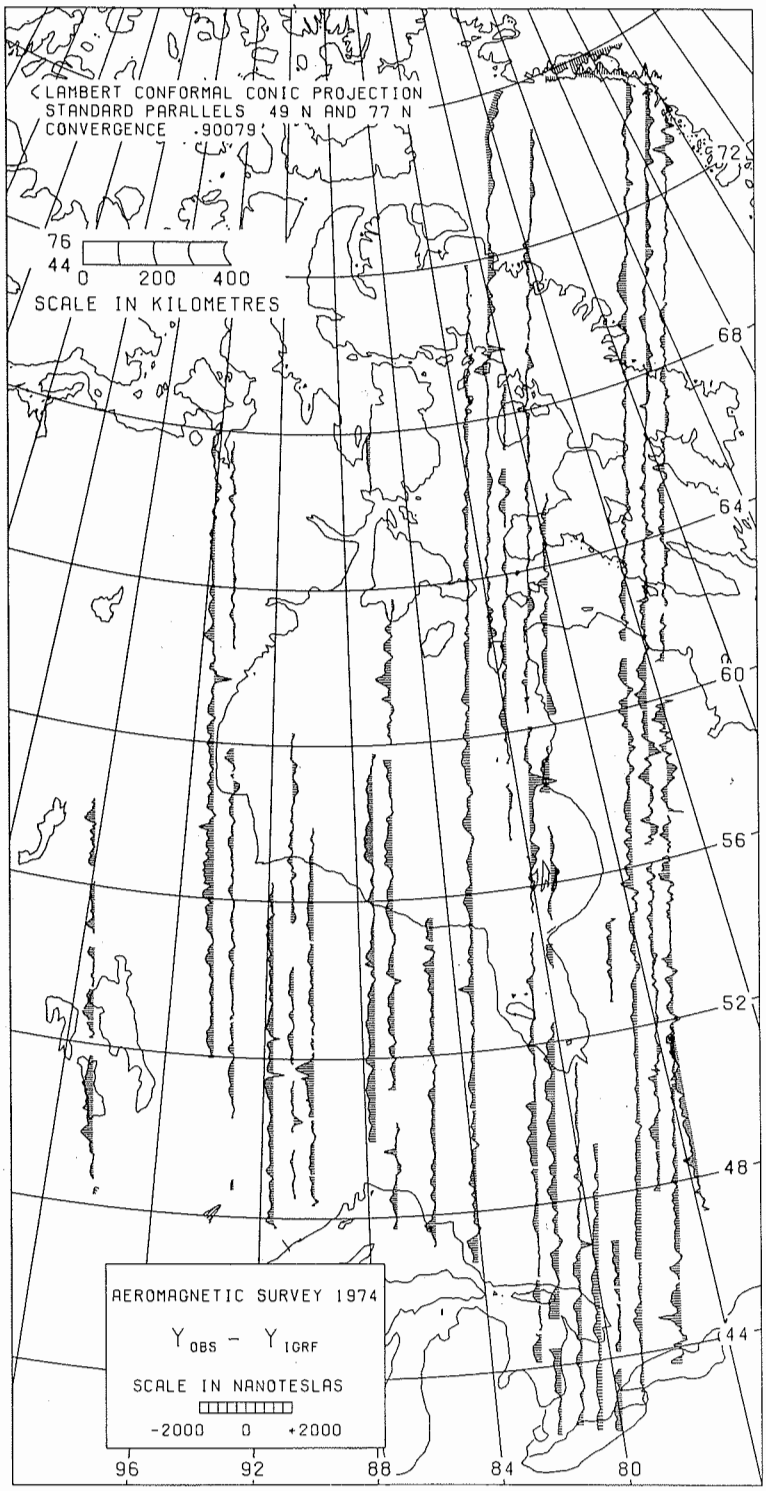

Figure 15. Residual profiles of geographic east component Y, relative to the IGRF, 1974.85.

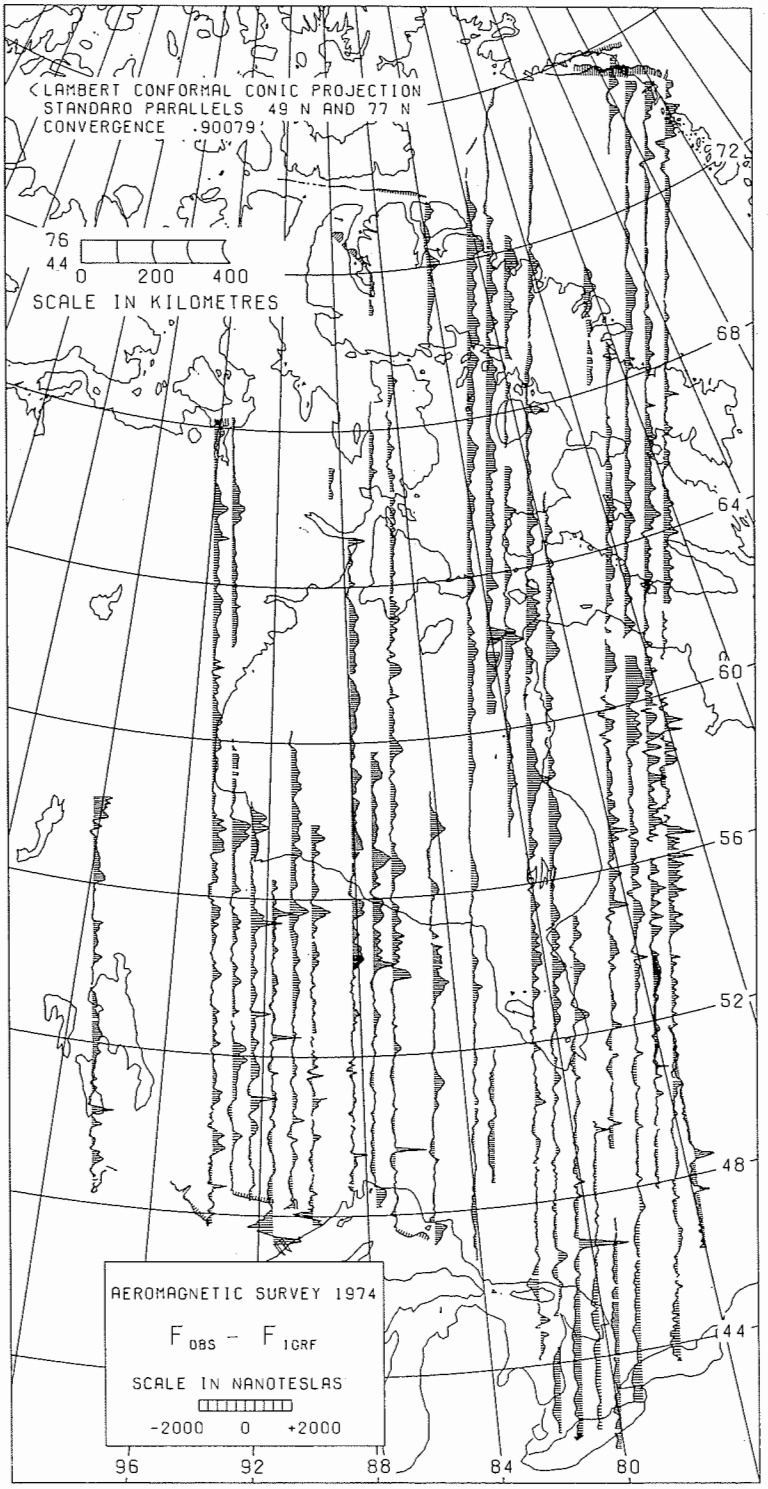

Figure 16. Residual profiles of total intensity F, relative to the IGRF, 1974.85.